Splice Strength of Conventional and High Relative Rib Area Bars in Normal and High-Strength Concrete

by Jun Zuo and David Darwin

The effects of concrete strength, coarse aggregate quantity and type, and reinforcing bar geometry on splice strength are evaluated. Results for 64 splice specimens with reinforcing bars with relative rib areas (ratio of projected rib area normal to bar axis to the product of the nominal bar perimeter and the center-to-center rib spacing) ranging from 0.069 to 0.141, concrete strengths ranging from 4250 to 15,650 psi (29 to 108 MPa), and quantities of limestone and basalt coarse aggregate ranging from 1586 to 1908 lb/yd³ (941 to 1132 kg/m³) are reported. The results are combined with the ACI Committee 408 database to develop design equations for development and splice length, which are then compared with the design criteria in ACI 318-99.

For splices not confined by transverse reinforcement, the 1/4 power of compressive strength f'_c best characterizes the effect of concrete strength on splice strength. $f'^{3/4}_c$ characterizes the effect of concrete strength on the additional splice strength provided by transverse reinforcement. The splice strength of bars confined by transverse reinforcement increases with an increase in relative rib area and bar diameter. The use of stronger coarse aggregate results in an increase in splice strength for bars both with and without confining reinforcement. For splices confined by transverse reinforcement, the higher the quantity of coarse aggregate, the greater the contribution of transverse reinforcement to splice strength. The expressions characterizing the splice strength of reinforcing bars accurately represent the development/splice strength of bottom-cast uncoated bars as a function of member geometry, concrete strength, relative rib area, bar size, and confinement, provided by both concrete and transverse reinforcement. The new design expressions are superior to the design criteria in ACI 318-99 in terms of both safety and economy. The criteria in ACI 318-99 for developed bars and Class A splices are unconservative for No. 6 (No. 19) and smaller bars.

Keywords: bond; deformed reinforcement; splice; stirrup; tie.

INTRODUCTION

Concrete properties have a significant effect on the bond strength between reinforcing bars and concrete. Azizinamini et al. (1993, 1995) studied the effect of high concrete strength on bond using beam splice tests. The test results indicated that the average bond stress at failure, normalized with respect to the square root of concrete compressive strength $\sqrt{f'_c}$, decreases with an increase in compressive strength. The rate of decrease becomes more pronounced as the splice length increases. Azizinamini et al. noted that the bearing capacity of concrete (related to f'_c) increases more rapidly than tensile strength (related to $\sqrt{f'_c}$) as compressive strength increases. For high-strength concrete, the higher bearing capacity prevents crushing of the concrete in front of the bar ribs (as occurs for normal strength concrete), which reduces local slip. They concluded that, because of the reduced slip, fewer ribs transfer load between the steel and the concrete, which increases the local tensile stresses and initiates a splitting failure in the concrete prior to achieving a uniform distribution of the bond force. Because of the brittle nature of these failures, they recommended that a minimum quantity of stirrups be used for bars spliced or developed in high-strength concrete.

Esfahani and Rangan (1996) investigated the influence of concrete strength on bond using both beam-end and splice tests. No confining transverse reinforcement was used. They observed that the extent of concrete crushing in front of ribs varied depending on concrete strength. As concrete strength increased, the degree of crushing decreased, with no concrete crushing observed for f'_c greater than 11,000 psi (75 MPa). In contrast to Azizinamini et al. (1993, 1995), they found that the average bond stress at failure, normalized with respect to the $\sqrt{f'_c}$, was higher for high-strength concrete than for normal strength concrete.

In work that preceded the current effort, Darwin et al. (1996a) noted that, for normal strength concretes, higher-strength coarse aggregates can increase the contribution of transverse reinforcement to bond strength by up to 45%. The scope of that study did not cover the effect of aggregate properties on bond in members without transverse reinforcement or the effect of aggregate quantity.

This paper describes the continuation of a study to improve the development characteristics of reinforcing steel by accurately characterizing the development and splice behavior of current reinforcing bars and modifying the deformation characteristics of bars to obtain improved bond strength. Earlier work in the study (Darwin and Graham 1993; Darwin et al. 1996a, 1996b) established that an increase in the relative rib area of reinforcing bars R_r (ratio of projected rib area normal to bar axis to the product of the nominal bar perimeter and the center-to-center rib spacing) increases the bond strength between reinforcing steel and concrete for bars confined by transverse reinforcement. The earlier work also demonstrated that an increase in R_r increases the bond strength of epoxy-coated reinforcement, both with and without confining steel.

RESEARCH SIGNIFICANCE

The principal goals of the work reported in this paper are to gain a better understanding of the effect of concrete properties on bond strength, to better understand the behavior of high relative rib area bars over the full range of concrete strengths now used in practice, and to develop a design expression that accurately represents the bond strength of reinforcing bars as a function of the geometric and material properties of the concrete member and the reinforcing bars.

*ACI member **Jun Zuo** is a structural engineer with Constructive Engineering Design, Kansas City, Mo. He received a BS in architectural engineering from Tongji University, China, and an MS and PhD in civil engineering from the University of Kansas, Lawrence, Kan.*

David Darwin, *FACI, is the Deane E. Ackers Professor of Civil Engineering and Director of the Structural Engineering and Materials Laboratory at the University of Kansas. He is a past member of the Board of Direction and the Technical Activities Committee and is past-president of the Kansas Chapter of ACI. He is also past-chairman of the Publications Committee and the Concrete Research Council, and a member and past-chairman of ACI Committee 224, Cracking. He chairs the TAC Technology Transfer Committee and ACI Committee 408, Bond and Development of Reinforcement, and serves on ACI Committees 446, Fracture Mechanics, and Joint ACI-ASCE Committees 445, Shear and Torsion; and 447, Finite Element Analysis of Reinforced Concrete Structures. He is a recipient of the Arthur R. Anderson and ACI Structural Research Awards.*

Only uncoated reinforcement is covered. The research is significant because it demonstrates that concrete strength has a much greater effect on the additional splice strength provided by transverse reinforcement than it does on the splice strength of bars not confined by transverse reinforcement. The paper also demonstrates that increases in aggregate strength and quantity result in higher splice strengths. Design expressions developed based on analyses of the test results and a large international database represent splice/development length as a function of concrete strength, relative rib area, bar size, and confinement provided by both concrete and transverse reinforcement. Of major significance is the observation that the design criteria in ACI 318-99 for developed bars and Class A splices are unconservative for No. 6 (No. 19) and smaller bars. Full details of the study are presented by Zuo and Darwin (1998).

EXPERIMENTAL PROGRAM

The test program consisted of 64 beam splice specimens containing uncoated, bottom-cast bars; 41 specimens had splices that were confined by stirrups, and 23 specimens had splices that were not confined by stirrups. Ten deformation patterns were evaluated. Reinforcing bars ranged in size from No. 5 to 11 (No. 16 to 36), with relative rib areas ranging from 0.69 to 0.141. Normal and high-strength concretes were manufactured with both limestone and basalt coarse aggregates. Concrete strengths ranged from 4,250 to 15,650 psi (29 to 108 MPa).

Test specimens

The splice specimens (Fig. 1) were 16 ft (4.9 m) long, with nominal widths of 12 or 18 in. (305 or 460 mm) and a nominal depth of 15.5 or 16 in. (395 or 405 mm). Splice lengths ranged from 16 to 40 in. (405 to 1020 mm). The beams contained two or three spliced bars (Fig. 1(a)) located in the constant moment region of simply supported test specimens. The beams were tested in an inverted position (Fig. 1(b)). Actual member dimensions are given in Table 1.

Materials

Reinforcing steel—The reinforcing bars met the requirements of ASTM A 615. Ten deformation patterns were evaluated, including four conventional patterns, designated 8C0A, 8N0, 11N0, and 11B0, and six experimental patterns, designated 5C3, 8C1, 8F1, 8N1, 8N3, and 11F3 (refer to Darwin et al. (1996a) for photographs of the deformation patterns). In the bar designations, the first number of the designation (one or two digits) is the bar size (customary units); the middle letter identifies the manufacturer; the trailing number identifies the deformation pattern; and a last letter is used if bars with the same deformation pattern were pro-
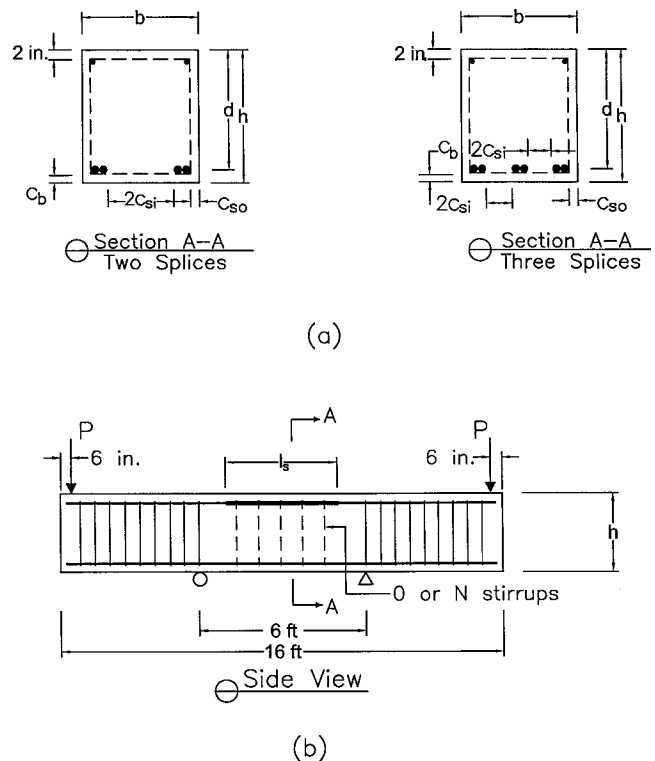

Fig. 1—Beam splice specimens: (a) beam configuration as cast; and (b) test setup (Note: 1 in. = 25.4 mm; 1 ft = 305 mm).

duced from different heats of steel. The relative rib areas range from 0.069 to 0.085 for the conventional bars and from 0.101 to 0.141 for high R_r bars. The reinforcing bars used as transverse reinforcement also met the requirements of ASTM A 615. Bar properties are given in Table 2.

Concrete—Six concrete mixtures were used to study the effects of concrete strength and type and quantity of coarse aggregate on splice strength. The mixtures are designated as NNL, NHL, HNL, HHL, NNB, and HHB, in which the first letter indicates the concrete strength, N = normal strength (f'_c < 8000 psi [55 MPa]), and H = high strength ($f'_c \geq 8000$ psi [55 MPa]); the second letter indicates the quantity of coarse aggregate, N = normal (1586 to 1661 lb/yd^3 [941 to 985 kg/m^3]), and H = high (1803 to 1908 lb/yd^3 [1070 to 1132 kg/m^3]); and the last letter indicates the type of coarse aggregate, L = limestone, and B = basalt. The limestone and basalt have compressive strengths of approximately 15,000 and 50,000 psi (103 and 345 MPa), respectively.

Concrete strengths ranged from 4250 to 6300 psi (29.3 to 43.4 MPa) for normal-strength concrete, and from 8370 to 15,650 psi (57.7 to 107.9 MPa) for high-strength concrete. Compressive strength was determined based on the average of at least three 6 x 12 in. (150 x 300 mm) cylinders for strengths lower than 12,500 psi (86 MPa) and at least three 4 x 8 in. (100 x 200 mm) cylinders for higher-strength concrete. Test ages ranged from 7 to 135 days. Mixture proportions and concrete properties are summarized in Table A.1 of Appendix A.[*]

Test procedure

The splice specimens were tested as shown in Fig. 1(b). Loads were applied at the ends of the cantilevered regions.

---

[*]The Appendix is available in xerographic or similar form from ACI headquarters, where it will be kept permanently on file, at a charge equal to the cost of reproduction plus handling at the time of request.

Table 1—Splice specimen properties and test results

Specimen no. and concrete*	Bar designation	n	l_s, in.	b, in.	h, in.	d_b, in.	c_{so}, in.	c_{si}, in.	c_b, in.	d, in.	f'_c, psi	N	d_s, in.	f_{yt}, ksi	P, kips	M_u, k-in.	f_s,[†] ksi
19.1 NNL	8N3	3	36	18.14	16.16	1.000	1.954	1.930	1.961	13.66	4250	0	—	—	38.18	2094.9	73.51
19.3 NNL	8N3	3	30	18.10	16.07	1.000	2.063	1.898	1.903	13.62	4250	3	0.375	64.55	37.02	2030.7	71.43
20.1 NNL	11F3	3	40	18.05	16.20	1.410	2.008	1.313	1.840	13.61	5080	8	0.500	84.70	69.84	3805.4	71.08
20.3 NNL	11F3	3	40	18.07	16.15	1.410	2.000	1.313	1.822	13.58	5080	5	0.500	84.70	67.30	3668.2	68.52
20.6 NNL	8N3	3	40	12.08	15.60	1.000	1.516	0.672	1.300	13.76	5080	0	—	—	29.61	1621	57.15
21.1 NNL	8N3	3	24	12.05	15.66	1.000	1.766	0.484	1.470	13.65	4330	6	0.625	62.98	37.27	2032.6	73.88
21.3 NNL	8N3	3	25	12.10	16.13	1.000	1.655	0.578	1.492	13.65	4330	5	0.625	62.98	38.43	2095.8	76.25
21.5 NNL	8N3	3	25	12.14	15.54	1.000	1.641	2.219	1.421	13.58	4330	5	0.500	64.92	26.67	1460.3	77.35
23a.1 HHL	8N3	3	21	18.28	16.09	1.000	2.164	1.852	1.931	13.62	9080	4	0.375	71.25	42.51	2325.9	78.87
23a.4 HHL	8N3	3	21	18.13	16.10	1.000	2.008	1.898	1.930	13.69	9080	4	0.375	71.25	42.88	2346.1	79.15
23a.5 HHL	8N3	2	22	18.19	16.16	1.000	2.000	1.891	1.938	13.63	9320	0	—	—	22.72	1247.9	62.24
23a.6 HHL	8N3	2	29	12.24	16.11	1.000	2.031	1.875	1.919	13.67	9320	0	—	—	27.25	1492.5	75.47
23b.1 HHL	8N3	3	18	12.15	16.22	1.000	1.469	0.711	1.951	13.73	8370	5	0.500	64.92	41.87	2281.3	79.04
23b.3 HHL	8N3	2	20	18.23	16.32	1.000	3.032	3.859	3.057	12.72	8370	0	—	—	24.02	1328.1	71.64
23b.5 HHL	11F3	2	25	12.03	16.24	1.410	2.032	1.125	1.939	13.56	4500	5	0.500	64.92	32.37	1954.3	54.80
24.1 NNL	8N1	2	32	12.14	16.12	1.000	2.000	1.875	1.903	13.69	4300	0	—	—	21.54	1184.9	61.91
25.1 NNL	5C3	3	17	12.19	16.27	0.625	1.985	1.023	1.556	14.37	4490	0	—	—	14.59	808.01	63.72
26.3 NNL	8N1	3	40	12.11	16.19	1.000	1.547	0.652	1.889	13.78	4960	0	—	—	32.34	1769.4	62.51
26.5 NNL	8N0	3	40	12.15	16.17	1.000	1.500	0.684	1.891	13.75	4960	0	—	—	33.21	1816.4	64.35
27.2 HHL	8N0	3	23	12.12	15.52	1.000	2.000	0.477	1.415	13.71	10810	6	0.375	64.92	42.70	2325.7	78.52
27.4 HHL	8N0	3	18	12.15	15.50	1.000	2.000	0.457	1.442	13.54	10810	5	0.500	64.92	40.78	2221.8	77.21
27.6 HHL	8N0	3	18	18.12	15.62	1.000	4.032	0.930	1.442	13.65	10810	4	0.500	64.92	43.02	2352.5	78.42
28.1 HHL	11F3	2	25	11.71	16.07	1.410	2.188	0.766	1.900	13.42	12,610	5	0.375	71.25	48.63	2646.2	71.23
28.3 HHL	11F3	3	28	18.10	16.09	1.410	2.172	1.242	1.901	13.45	12,610	4	0.375	71.25	68.89	3751.7	67.03
28.5 HHL	11F3	2	30	18.09	16.20	1.410	1.977	4.031	1.999	13.45	12,610	0	—	—	35.40	1944	50.89
29.2 HHB	8N0	3	20	12.14	15.60	1.000	1.875	0.484	1.478	13.60	10,620	5	0.375	71.25	46.07	2507.7	83.65
29.4 HHB	8N0	3	18	12.17	15.60	1.000	1.938	0.492	1.418	13.66	10,620	6	0.375	71.25	41.94	2284.4	77.96
29.6 HHB	8N0	3	16	18.17	15.65	1.000	3.906	0.980	1.414	13.71	10,620	4	0.375	71.25	42.25	2310.8	77.72
30.1 HHB	11F3	2	25	12.19	16.15	1.410	2.375	0.688	1.891	13.51	13,220	3	0.375	71.25	45.63	2484.8	66.07
30.3 HHB	11F3	3	28	18.02	16.11	1.410	1.953	1.273	1.889	13.47	13,220	2	0.375	71.25	68.97	3755.7	66.88
30.5 HHB	11F3	2	30	18.12	16.15	1.410	2.063	4.016	1.956	13.44	13,220	0	—	—	46.72	2554.9	66.95
31.3 HHB	8N0	2	16	12.15	15.48	1.000	1.969	1.938	1.438	13.52	12,890	2	0.375	71.25	23.39	1282.4	65.21
31.5 HHB	8N1	3	22	12.26	15.58	1.000	1.828	0.508	1.494	13.56	12,890	0	—	—	32.73	1787.4	61.43
31.6 HHB	8C0A	3	22	12.17	15.49	1.000	1.719	0.539	1.492	13.44	12,890	0	—	—	33.47	1826.9	63.42
32.1 HHB	11F3	2	32	12.17	16.17	1.410	2.000	0.984	1.904	13.52	14,400	0	—	—	43.86	2390.4	63.33
32.2 HHB	11B0	2	32	12.14	16.16	1.410	2.000	1.063	1.916	13.51	14,400	0	—	—	42.55	2319.3	61.49
32.3 HHB	11F3	2	32	18.14	16.15	1.410	1.969	4.016	1.947	13.45	14,400	0	—	—	42.41	2322.6	60.64
32.4 HHB	11B0	2	28	18.20	16.17	1.410	2.031	4.047	1.935	13.50	14,400	0	—	—	42.85	2345.7	61.01
33.2 NHL	8C0A	3	18	12.10	16.12	1.000	1.953	0.395	1.913	13.66	5360	6	0.500	64.92	31.69	1731.7	61.42
33.3 NHL	8N1	3	18	18.14	16.13	1.000	2.070	1.918	1.969	13.63	5360	4	0.375	71.25	30.27	1664.6	57.60
33.4 NHL	8C0A	3	18	18.12	16.13	1.000	2.063	1.914	1.936	13.64	5360	4	0.375	71.25	30.67	1686.7	58.32
33.6 NHL	8C0A	3	22	12.17	16.26	1.000	2.094	1.688	1.891	13.82	5230	2	0.375	71.25	20.57	1131.6	57.94
34.3 NHL	8C0A	3	24	18.12	16.02	1.000	2.080	1.844	1.981	13.49	5440	0	—	—	30.64	1685.2	58.94
35.1 NNL	8F1	2	20	12.08	16.17	1.000	1.453	2.375	1.938	13.69	5330	5	0.375	71.25	24.08	1320.9	68.44
35.3 NNL	8C0A	2	20	12.08	16.07	1.000	1.500	2.266	1.920	13.60	5330	5	0.375	71.25	21.58	1185.7	61.77
36.3 NHL	8C0A	3	26	18.17	16.10	1.000	2.016	1.836	2.000	13.55	5060	0	—	—	32.68	1796.3	62.78
37.4 NNL	8F1	3	21	12.07	15.51	1.000	2.000	0.484	1.503	13.47	4800	7	0.500	64.92	37.02	2018.7	73.78
38.2 NNL	8C0A	3	26	18.17	16.14	1.000	2.125	1.844	2.075	13.51	5080	0	—	—	31.41	1727.8	60.51
39.2 HHB	8C1	3	16	12.18	15.48	1.000	1.906	0.516	1.475	13.49	14,450	4	0.375	71.25	38.59	2103.2	69.74
39.3 HHB	8N0	3	16	12.17	15.45	1.000	1.891	0.488	1.477	13.45	14,450	4	0.375	71.25	41.43	2256.5	77.96
39.6 HHB	8C1	3	21	12.19	15.41	1.000	1.953	0.508	1.505	13.59	14,450	0	—	—	36.10	1969.1	67.38
40.1 HHB	11F3	2	23	12.16	15.48	1.410	2.031	1.000	1.473	13.26	15,650	4	0.375	71.25	45.38	2470.5	66.60
40.4 HHB	11N0	2	23	12.09	15.52	1.410	2.000	1.063	1.451	13.33	15,650	4	0.375	71.25	40.32	2197.1	58.83

*Specimen and concrete: G.P-SQA = group number (19 to 43); P = casting order in group (1 to 6); S = strength (N = normal, H = high); Q = aggregate quantity (N = normal, H = high); and A = aggregate type (L = limestone, B = basalt).

[†]Bar stress computed using moment-curvature method if M_u does not exceed moment capacity from moment-curvature analysis; otherwise, f_s computed using ultimate strength method; M_u and f_s include effects of beam self-weight and loading system.

Note: N = number of stirrups; d_s = stirrup diameter; f_{yt} = stirrup yield strength; 1 in. = 25.4 mm; 1 psi = 6.89 kPa; 1 ksi = 6.89 MPa; 1 kip = 4.45 kN; and 1 k-in. = 0.113 kN-m.

Table 1 (cont.)—Splice specimen properties and test results

Specimen no. and concrete[*]	Bar designation	n	l_s, in.	b, in.	h, in.	d_b, in.	c_{so}, in.	c_{si}, in.	c_b, in.	d, in.	f'_c, psi	N	d_s, in.	f_{yt}, ksi	P, kips	M_u, k-in.	f_s,[†] ksi
40.5 HHB	8N0	2	17	12.11	16.04	1.000	2.000	1.875	1.846	13.67	15,650	0	—	—	24.00	1315.9	65.81
41.1 HHL	8N3	2	16	12.14	15.55	1.000	2.000	1.844	1.522	13.49	10,180	2	0.375	71.25	23.52	1289.5	66.16
41.2 HHL	8N3	3	16	12.16	15.53	1.000	1.875	0.469	1.515	13.38	10,180	4	0.625	62.98	44.34	2413.6	83.02
41.3 HHL	8N3	3	16	12.11	16.09	1.000	1.891	0.461	1.890	13.56	10,180	4	0.500	64.92	41.87	2280.9	79.35
41.4 HHL	8N0	3	16	12.20	15.53	1.000	1.906	0.484	1.476	13.40	10,180	4	0.625	62.98	40.28	2194.4	77.27
41.6 HHL	8C0A	3	16	18.22	16.17	1.000	2.000	1.875	1.984	13.63	10,500	2	0.375	71.25	35.26	1934.3	65.38
42.1 HNL	8N0	2	16	12.11	15.99	1.000	2.000	1.859	1.864	13.50	11,930	2	0.375	71.25	22.97	1260.1	64.32
42.4 HNL	8N0	3	16	12.17	16.09	1.000	1.906	0.500	1.829	13.74	11,930	4	0.500	64.92	38.07	2075.9	70.70
42.5 HNL	8N0	3	16	12.18	15.36	1.000	1.906	0.500	1.476	13.62	11,930	4	0.625	62.98	41.60	2266.0	77.92
43.2 HNL	8N3	2	16	12.06	16.06	1.000	2.031	1.875	1.844	13.68	11,530	2	0.375	71.25	23.49	1288.5	64.95
43.3 HNL	8N3	3	16	12.22	16.07	1.000	1.844	0.500	1.859	13.83	11,530	4	0.500	64.92	42.70	2326.4	78.81
43.6 HNL	8N3	3	16	12.07	15.48	1.000	1.891	0.500	1.492	13.62	11,530	4	0.625	62.98	45.16	2458.3	82.73

[*]Specimen and concrete: G.P-SQA = group number (19 to 43); P = casting order in group (1 to 6); S = strength (N = normal, H = high); Q = aggregate quantity (N = normal, H = high); and A = aggregate type (L = limestone, B = basalt).

[†]Bar stress computed using moment-curvature method if M_u does not exceed moment capacity from moment-curvature analysis; otherwise, f_s computed using ultimate strength method; M_u and f_s include effects of beam self-weight and loading system.

Note: N = number of stirrups; d_s = stirrup diameter; f_{yt} = stirrup yield strength; 1 in. = 25.4 mm; 1 psi = 6.89 kPa; 1 ksi = 6.89 MPa; 1 kip = 4.45 kN; and 1 k-in. = 0.113 kN-m.

Table 2—Properties of reinforcing bars

Bar designation[*]	Yield strength, ksi	Nominal diameter, in.	Weight, lb/ft	% light or heavy	Rib spacing, in.	Rib height		Relative rib area
						ASTM, in.	Average,[†] in.	
5C3	62.98	0.625	1.033	1.0%L	0.258	0.047	0.043	0.141
8C0A	69.50	1.000	2.615	2.1%L	0.598	0.066	0.063	0.085
8N0	77.96	1.000	2.594	2.8%L	0.650	0.057	0.054	0.069
8C1	67.69	1.000	2.592	5.3%L	0.504	0.064	0.060	0.101
8F1	75.42	1.000	2.600	2.6%L	0.471	0.078	0.074	0.140
8N1	79.70	1.000	2.733	2.4%H	0.441	0.073	0.068	0.121
8N3	80.57	1.000	2.730	2.2%H	0.487	0.072	0.068	0.119
11N0	65.54	1.410	5.157	2.9%L	0.911	0.079	0.075	0.072
11B0	66.69	1.410	5.102	4.0%L	0.825	0.070	0.066	0.070
11F3	77.77	1.410	5.145	3.2%L	0.615	0.090	0.088	0.127

[*]Bar designation: No. AAB, No. = bar size (No. 5, No. 8, or No. 11); AA = bar manufacturer and deformation pattern; B0 = conventional Birmingham Steel bars; C0 = conventional Chapparal Steel bars; C1, C3 = new Chapparal Steel bars; N0 = conventional North Star Steel bars; F1, F3 = new Florida Steel bars; N1, N3 = new North Star Steel bars; B = letter used if bar had same deformation pattern as reported by Darwin et al. (1996a), but were produced from different steel heat.

[†]Average rib height between longitudinal ribs.

Note: 1 in. = 25.4 mm; 1 ksi = 6.89 MPa; 1 lb/ft = 1.49 kg/m; and 1 mil = 0.0254 mm.

Beams were loaded continuously at a rate of approximately 3 kips (13.3 kN) per min until failure, with tests lasting 15 to 20 min.

SPECIMEN BEHAVIOR AND ANALYSIS OF TEST RESULTS
Results and observations

Moments and maximum bar stresses in the splices at failure are given in Table 1. The effects of beam self-weight and the weight of the loading system are included. Bar stresses are calculated using moment-curvature or ultimate strength methods, as indicated in Table 1 and described in Appendix B.[*]

Most of the specimens failed by splitting at the tension face within the splice region. For members cast with normal strength concrete, beams with splices that were not confined by transverse stirrups failed suddenly, with a quick drop in load after the peak. Beams with splices confined by stirrups exhibited a more ductile behavior, with a slow drop in load after the peak. For members cast with high-strength concrete, similar differences were observed between members without

and with stirrups. The high-strength concrete beams failed in a more brittle manner than the normal-strength concrete beams.

The extent of concrete damage at the steel-concrete interface depended on the concrete strength and bar deformation pattern. Damage was more extensive near the discontinuous ends of splices. For normal strength concrete, damage was similar to that observed by Darwin et al. (1996a)—for conventional bars, the concrete crushed between the bar ribs, while for high R_r bars, the concrete both crushed and sheared. In general, the greater the confinement provided by transverse reinforcement, the greater the damage at the interface near the discontinuous ends of the spliced bars.

For high-strength concrete specimens without stirrups in the splice region, the interface showed little or no concrete damage. For bars confined by stirrups, concrete damage at the interface was similar to that observed in normal strength concrete beams, but the damage occurred over a longer region, up to 3/4 of the splice length.

In matched pairs of specimens containing conventional and high relative rib area bars confined by stirrups, the high relative rib area bars produced higher splice strengths.

[*]The Appendix is available in xerographic or similar form from ACI headquarters, where it will be kept permanently on file, at a charge equal to the cost of reproduction plus handling at the time of request.

Table 3—Effect of concrete properties on splice strength of splices not confined by transverse reinforcement

Concrete[*]	Number of tests	Test-prediction ratio[†]		
		Maximum	Minimum	Average
NNL	35	1.25	0.90	1.00
NHL	6	1.06	0.98	1.01
HHL	4	1.00	0.88	0.96
NNB	2	1.15	1.06	1.11
HHB	9	1.27	0.99	1.13

[*]Concrete designation: SQA: S = strength (N = normal, H = high); Q = aggregate quantity (N = normal, H = high); and A = aggregate type (L = limestone, B = basalt).
[†]Test-predicted splice strength ratio; test strength = $A_b f_s / f_c'^{1/4}$, determined from test results; predicted strength determined using Eq. (1); and predicted strengths for individual specimens presented in Table A.5 of Appendix A.

Evaluation of test results

In previous work on high R_r bars, Darwin et al. (1996a) observed that the type of coarse aggregate significantly affects splice strength for bars that are confined by stirrups. That study did not address the effect of coarse aggregate type on the splice strength of bars not confined by transverse reinforcement nor the effect of coarse aggregate quantity.

Darwin et al. (1996b) found that the 1/4 power of the concrete compressive strength f_c' characterizes the effect of concrete strength on splice strength for bars both confined and not confined by transverse reinforcement. The earlier studies (Darwin et al., 1996a) also showed that the additional strength provided by confining steel T_s, normalized with respect to $f_c'^{1/4}$, is a function of the effective transverse reinforcement NA_{tr}/n, in which N is the number of transverse stirrups or ties in the splice region, A_{tr} is the area of each stirrup or tie crossing the potential plane of splitting adjacent to the reinforcing bars being developed or spliced, and n is the number of reinforcing bars being developed or spliced along the plane of splitting. The yield strength of the transverse reinforcement was found to have no measurable effect on T_s (Maeda et al. 1991; Sakurada et al. 1993; Azizinamini et al. 1995; and Darwin et al. 1996a, 1996b). The database used by Darwin et al., however, included only a small number of specimens made with high-strength concrete. Thus, with more data available on high-strength concrete specimens, the question arises as to whether or not the 1/4 power of f_c' is still appropriate for characterizing the contribution of concrete strength to bond.

For the evaluations that follow, the current results are combined with those reported by Choi et al. (1991), Hester et al. (1993), and Darwin et al. (1996a) on splice specimens similar to the current NNL concrete specimens (normal strength concrete with a normal quantity of limestone coarse aggregate). Specimens 8.3 and 10.5 tested by Darwin et al. (1996a) contained NNB concrete (B = Basalt). The previous test results are summarized in Tables A.2, A.3, and A.4 of Appendix A.[*] Strength evaluations are based on the assumption that the total force in a bar at splice failure T_b equals the sum of a concrete contribution T_c and a transverse reinforcement (steel) contribution T_s, $T_b = T_c + T_s$.

Concrete contribution T_c—Using procedures described by Darwin et al. (1996b) and a database consisting of 171 specimens containing developed or spliced bars not confined by transverse reinforcement (Chinn 1955; Chamberlin 1956, 1958; Ferguson and Breen 1965; Thompson et al. 1975; Zekany et al. 1981; Choi et al. 1991; Hester et al. 1993; Rezansoff et al. 1993; Azizinamini et al. 1993; Hatfield et al. 1996; Darwin et al. 1996a; Zuo and Darwin 1998) with concrete

strengths ranging from 2610 to 15,650 psi (18.0 to 107.9 MPa), the ultimate bond force for bars not confined by transverse reinforcement T_c can be expressed as (Zuo and Darwin 1998)

$$\frac{T_c}{f_c'^{1/4}} = \frac{A_b f_s}{f_c'^{1/4}} = [59.8 l_d (c_{min} + 0.5 d_b) + 2350 A_b]$$

$$\left(0.1 \frac{c_{max}}{c_{min}} + 0.9\right)$$ (1)

where

A_b	=	single spliced bar area, in.[2];
f_s	=	bar stress at failure, psi;
f_c'	=	concrete compressive strength, psi; $f_c'^{1/4}$, psi
l_d	=	splice or development length, in.;
c_{min}, c_{max}	=	minimum or maximum value of c_s, or c_b ($c_{max}/c_{min} \leq 3.5$), in.;
c_s	=	min ($c_{si} + 0.25$ in., c_{so}) in.;
c_{si}	=	1/2 of clear spacing between bars, in.;
c_{so}, c_b	=	side or bottom cover of reinforcing bars, in.; and
d_b	=	bar diameter, in.

This expression differs somewhat from that obtained in the earlier studies (Darwin et al. 1996a, 1996b) in that the coefficient for l_d has decreased from 63 to 59.8 and the coefficient for A_b has increased from 2130 to 2350. As before, $f_c'^{1/4}$ best represents the effect of compressive strength bond strength. The database used to establish Eq. (1) includes an additional 38 beams, compared to that used by Darwin et al. (1996b), and an increase from 7 to 19% in the portion of the tests representing high-strength concrete ($f_c' > 8000$ psi [55 MPa]). A comparison of the test and predicted strengths for the beams used to establish Eq. (1) is presented in Table A.5 of Appendix A.[*] The mean test-prediction ratio is 1.00, with a coefficient of variation (COV) of 0.104, compared to 1.00 and 0.107 obtained by Darwin et al. (1996b) for the smaller database. Test-prediction ratios based on Eq. (1) are used to evaluate the effects of concrete properties on splice strength.

Effects of concrete properties on splices without transverse reinforcement

Specimens without stirrups within the splice region include 35 containing NNL concrete (nine from the current study, 12 from Darwin et al. [1996a], eight from Choi et al. [1991], and seven from Hester et al. [1993]), two containing NNB concrete (Darwin et al. 1996a), six containing NHL concrete, four containing HHL concrete, and nine containing HHB concrete.

Effect of coarse aggregate—Table 3 summarizes the range and mean of the test-prediction ratios for the splices not confined by stirrups. The results show no measurable difference in the test-prediction ratios for concrete containing the same type of coarse aggregate, regardless of coarse aggregate content or concrete strength, but do show a difference based on the type of coarse aggregate. The average test-prediction ratios range from 0.96 to 1.01 for the concretes containing limestone, compared with 1.10 and 1.13 for the concretes containing basalt. This observation can be explained based on studies by Kozul and Darwin (1997) and Barham and Darwin (1999), using the same coarse aggregates, which show that concretes containing basalt yield only slightly higher flexural

---

[*]The Appendix is available in xerographic or similar form from ACI headquarters, where it will be kept permanantly on file, at a charge equal to the cost of reproduction plus handling at the time of request.
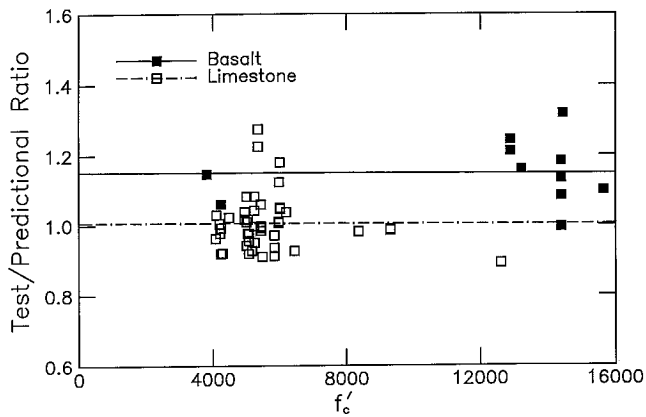
Fig. 2—Test-prediction ratio versus concrete compressive strength f_c' for splices not confined by transverse reinforcement in concrete containing basalt and limestone coarse aggregates, using dummy variable analysis based on type of coarse aggregate (1 psi = 6.89 kPa).

Fig. 3—Increase in bond force T_s normalized with respect to $f_c'^{1/4}$ versus t_rNA_{tr}/n for No. 8 (No. 25) conventional bars in normal (N) and high-strength (H) concrete containing normal (N) quantities of limestone (L) coarse aggregate, showing contributions to splice strength as function of concrete strength and quantity of coarse aggregate (1 in. = 25.4 mm).

Fig. 4—Increase in bond force T_s normalized with respect to $f_c'^{1/4}$ versus NA_{tr}/n for No. 8 (No. 25) conventional bars in normal (N) and high-strength (H) concrete containing normal (N) quantities of coarse aggregate, as affected by coarse aggregate type (basalt [B] or limestone [L]) and relative rib area (1 in. = 25.4 mm).

strengths but significantly higher fracture energies (more than two times higher) than concrete of similar compressive strength containing limestone for all compressive strengths evaluated (2920 to 14,320 psi [20 to 99 MPa]). The higher fracture energy provided by the basalt results in an increased resistance to crack propagation that delays splitting failure and increases splice strength.

Effect of concrete strength—Figure 2 compares test-prediction ratios to concrete strength for splice specimens containing limestone and basalt coarse aggregate. The best-fit lines are based on a dummy variable regression analysis that limits the effect of the different number of tests carried out for normal and high-strength concrete with each aggregate. The best-fit lines are nearly horizontal, and the intercept of the line for specimens containing basalt is approximately 15% greater than that for the specimens containing limestone.

Because the predictions used are based on Eq. (1), these observations illustrate that, on average for the specimens shown, $f_c'^{1/4}$ provides an unbiased representation of the effect of concrete strength on bond and, as demonstrated in Table 3, stronger coarse aggregates produce higher splice strengths. A comparison of test/prediction ratio versus f_c' for all 177 specimens used to develop Eq. (1) also produces a horizontal best-fit line (Zuo and Darwin, 1998). In contrast, if Eq. (1) is replaced by an expression based on $\sqrt{f_c'}$, the best-fit lines (for both the data shown in Fig. 2 and the full database) slope sharply down, indicating that such a relationship progressively overpredicts bond strength as f_c' increases.

Effects of concrete properties on splices with transverse reinforcement

To investigate the effects of concrete properties on the strength of splices confined by transverse reinforcement, the additional bond force due to confinement provided by transverse reinforcement T_s is obtained by subtracting T_c (calculated using Eq. (1)) from the experimentally determined total bond force T_b. Initially, comparisons of $T_s/f_c'^{1/4}$ with NA_{tr}/n are used to evaluate the effect of concrete properties on T_s for the specimens tested in this study, plus those tested by Hester (1993) and Darwin et al. (1996a).

Effect of coarse aggregate—Figure 3 compares $T_s/f_c'^{1/4}$ versus t_rNA_{tr}/n for No. 8 (No. 25) conventional bar splices in normal and high-strength concretes containing normal and high quantities of limestone coarse aggregate. The term $t_r = 9.6 R_r + 0.28$ (Darwin et al. 1996a) represents the observed
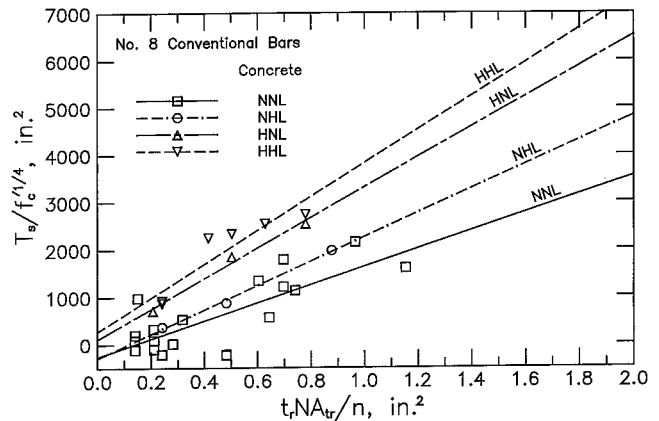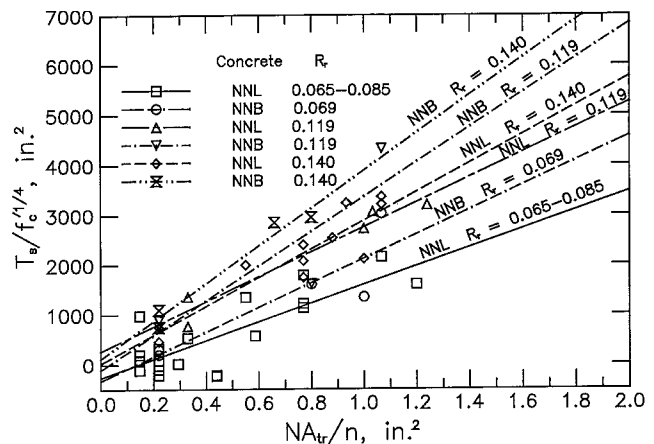
effect of relative rib area on T_s. Using t_r as a parameter eliminates the effect of small differences in relative rib area (R_r ranges from 0.065 to 0.085) from the analysis.

Figure 3 shows that $T_s/f_c'^{1/4}$ is higher for concretes containing high quantities of coarse aggregate (NHL and HHL) than for the concretes containing normal quantities (NNL and HNL), demonstrating that the quantity of coarse aggregate can have a measurable effect on T_s.

$T_s/f_c'^{1/4}$ is compared with NA_{tr}/n in Fig. 4 for conventional and high R_r No. 8 (No. 25) bars cast in normal strength concretes containing normal quantities of limestone and basalt coarse aggregate. Note that t_r is not used as a parameter in this comparison. The figure shows that $T_s/f_c'^{1/4}$ is higher, the higher the relative rib area of the bar. The figure also shows that, for all bar patterns, $T_s/f_c'^{1/4}$ is higher for concrete containing basalt than for concrete containing limestone, matching the earlier observations (Darwin et al. 1996a). Similar results are obtained in the current study for bars cast in high-strength concrete (Zuo and Darwin 1998).
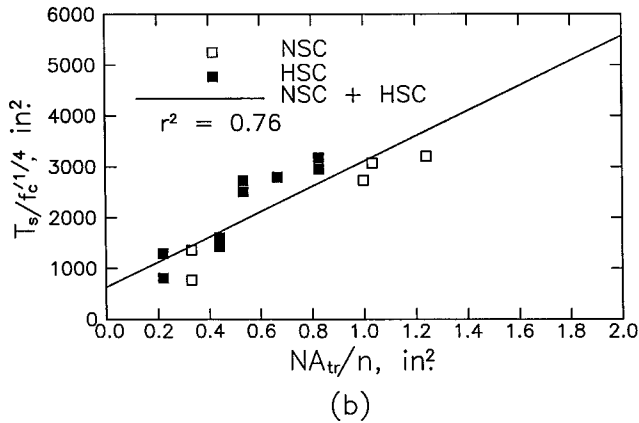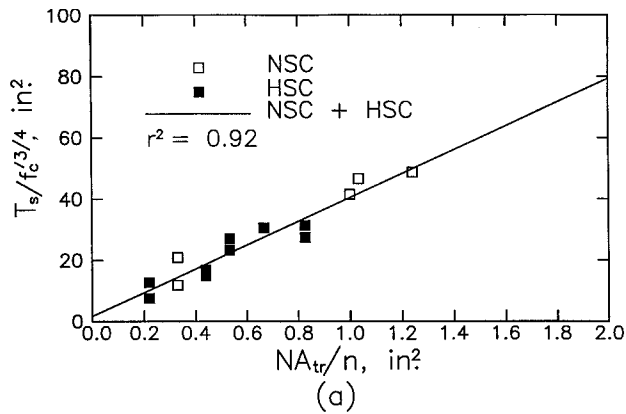
Fig. 5—*Increase in bond force due to transverse reinforcement* T_s *normalized with respect to* $f_c'^{\,p}$ *versus* NA_{tr}/n *for No. 8 (No. 25) high relative rib area bars (8N3): (a)* p = 3/4; *and (b)* p = 1/4 (1 in. = 25.4 mm).

Effect of concrete strength for current tests—Figure 3 shows that, for conventional bars, $T_s/f_c'^{\,1/4}$ is higher for high-strength concrete than for normal strength concrete. Similar results are obtained for high R_r bars (Zuo and Darwin 1998). These observations indicate that a power of f_c' greater than 1/4 is needed to accurately characterize the effect of concrete strength on T_s.

To capture what might be referred to as the main behavior, powers p of f_c' equal to 1/4, 1/2, 3/4, and 1.0 were evaluated. To limit the number of variables, comparisons were initially made only for members containing limestone coarse aggregate. The test results for No. 8 and 11 (No. 25 and 36) high R_r bars, 8N3 (R_r = 0.119) and 11F3 (R_r = 0.127), and No. 8 (No. 25) conventional bars were used for this purpose. For each bar, T_s normalized with respect to $f_c'^{\,p}$ is plotted versus NA_{tr}/n, as illustrated for 8N3 bars and two values of p in Fig. 5a and 5b. The best-fit lines for each value of p are then determined.

In general, the closer the coefficient of determination r^2 is to 1.0 for a best-fit line, the better the correlation between $T_s/f_c'^{\,p}$ and NA_{tr}/n, which, in turn, indicates the better value of p to characterize the effect of concrete strength on T_s. The values of r^2 for the different values of p are summarized in Table 4. The results show that p = 3/4 produces the highest r^2 for the high R_r bars: r^2 = 0.92 for 8N3 bars, and r^2 = 0.66 for 11F3 bars. p = 1.0 produces the highest r^2 (0.71) for the conventional No. 8 (No. 25) bars. For all three bar patterns, p = 1/4 produces the lowest r^2 values (0.76 for 8N3 bars, 0.57 for 11F3 bars, and 0.48 for conventional No. 8 [No. 25] bars).

Table 4—Coefficients of determination r^2 for best-fit lines of T_s/f_c' versus NA_{tr}/n for high relative rib area and conventional bars

Bar designation[*]	No. of tests		r^2			
	NSC[†]	HSC[‡]	p = 1/4	p = 1/2	p = 3/4	p = 1
Conventional No. 8	23	9	0.48	0.58	0.66	0.71
8N3	5	10	0.76	0.90	0.92	0.87
11F3	11	2	0.57	0.63	0.66	0.66

[*]Notation of bar designation is same as in Table 2.
[†]Normal strength concrete containing coarse aggregate; f_c' < 8000 psi.
[‡]High-strength concrete containing limestone coarse aggregate; 8000 psi ≤ f_c' < 16,000 psi.
Note: 1 psi = 6.895 kPa.

Table 5—C_1, C_2, t_r, t_d, and r^2 for different values of p

p^*	C_1	C_2	t_r	t_d	$r^{2\dagger}$
1/4	1977	455	7.9 R_r + 0.41	0.87 d_b + 0.13	0.787
1/2	247	40.4	8.8 R_r + 0.34	0.83 d_b + 0.17	0.836
3/4	30.9	3.59	9.6 R_r + 0.28	0.78 d_b + 0.22	0.858
1.0	3.823	0.322	10.3 R_r + 0.23	0.73 d_b + 0.27	0.860

[*]Power of concrete compressive strength f_c' used to normalize additional bond force provided by transverse reinforcement T_s.
[†]Coefficient of determination of best-fit line.

$T_s/f_c'^{\,p}$ for 8N3 bars is plotted versus NA_{tr}/n in Fig. 5(a) and (b) for p = 3/4 and 1/4, respectively. The figures show that when T_s is normalized with respect to $f_c'^{\,3/4}$, the data points for high-strength and normal strength concrete overlap, resulting in a higher value of r^2. When T_s is normalized with respect to $f_c'^{\,1/4}$, the normalized bond forces are higher for high-strength concrete than for normal strength concrete.

Effect of concrete strength using database—Overall, the best power of f_c' to characterize the effect of concrete strength on T_s involves consideration of two other variables: bar diameter d_b, and relative rib area R_r. Following procedures used by Darwin et al. (1996a), an analysis was performed (Zuo and Darwin 1998) with a database consisting of 163 development and splice tests from the U.S. and Canada (Mathey and Watstein 1961; Ferguson and Breen 1965; Thompson et al. 1975; Zekany et al. 1981; DeVries et al. 1991; Hester et al. 1993; Rezansoff et al. 1991, 1993; Azizinamini 1995; Darwin et al. 1996a; and Zuo and Darwin 1998). The linear relationships producing the best match with the data for each value of p are expressed as

$$\frac{T_s}{f_c'^{\,p}} = C_1(t_r t_d)\frac{NA_{tr}}{n} + C_2 \qquad (2)$$

The coefficients, C_1, C_2, t_r, and t_d, and the coefficients of determination r^2 are summarized in Table 5 for the four values of p. In each case, t_r increases linearly with relative rib area, and t_d increases linearly with bar diameter. r^2 is highest (0.860) for p = 1.0. r^2 (0.858) is just slightly lower for p = 3/4. p = 1/4 produces the lowest value of r^2 (0.786).

As the next step, for each value of p, Eq. (2) is combined with Eq. (1) to obtain predicted strengths. The predicted strengths and test-prediction ratios for the 163 specimens are summarized in Table A.6 of Appendix A.[*] The average of the test-prediction

[*]The Appendix is available in xerographic or similar form from ACI headquarters, where it will be kept permanantly on file, at a charge equal to the cost of reproduction plus handling at the time of request.

ratios is 1.0 for all four values of p. The least scatter in the results, as indicated by the COV, is obtained for $p = 1/2$, for which the COV = 0.116. $p = 3/4$ and $p = 1/4$ provide COVs of 0.120 and 0.122, respectively; while $p = 1.0$ has the highest COV (0.132). The values of COV reflect the accuracy of the predictions for the overall database, while the values of r^2 reflect the goodness of fit between each expression and the data.

The best value of p for characterizing the effect of concrete strength on T_s should provide not only a low COV and a high r^2, but unbiased predictions for both normal and high-strength concrete. This means that, for the appropriate value of p, the best-fit line of the test-prediction ratio versus f'_c should be horizontal. The best-fit lines for the four values of p are plotted in Fig. 6(a). The figure shows that the slope of the lines decreases with an increase in the value of the power of p. $p = 3/4$ gives the smallest positive slope and a line that is nearly horizontal, while $p = 1.0$ gives a negative slope. Thus, of the four values of p, $p = 3/4$ gives the least biased predictions of bond strength based on concrete strength. $p = 1.0$ overestimates bond strength for bars in high-strength concrete. The results in Fig. 6(a) suggest that the best value of p may be slightly higher than 0.75.

As another check on the value of p and the accuracy of Eq. (1) and (2), an independent set of 33 splice specimens tested by Kadoriku (1994) was analyzed. For this series, f'_c ranged from 3070 to 10,980 psi (21.2 to 75.7 MPa), and a single bar diameter of 19 mm was used. Because R_r was not reported, a value of R_r = 0.748 (the mean value for No. 6 [19 mm] conventional bars [Darwin 1996b]) is used. The analysis (summarized in Table A.7 of Appendix A[*]) indicates that $p = 3/4$ provides the lowest COV (0.085) for the 33 specimens. The best-fit lines for test-prediction ratios using the four values of p are plotted versus f'_c in Fig. 6(b), and show the same characteristics as in Fig. 6(a): $p = 3/4$ provides a nearly horizontal line, with the smallest positive slope, while $p = 1.0$ gives a negative slope. Thus, among the values of p evaluated, $p = 3/4$ is the most appropriate for use in characterizing the effect of concrete strength on T_s. For simplicity and convenience, $p = 3/4$, (rather than a possibly more precise, slightly higher value) is selected for the next step.

DESIGN EXPRESSIONS

To take full advantage of the data available, the 33 tests by Kadoriku (1994) are combined with the initial 163 tests to obtain a best-fit expression for the contribution of transverse reinforcement to splice strength

$$\frac{T_s}{f_c'^{3/4}} = 31.14 t_r t_d \frac{NA_{tr}}{n} + 3.99 \tag{3}$$

with $r^2 = 0.856$.

Combining Eq. (1) with (3) gives an expression for total bond force

$$\frac{T_b}{f_c'^{1/4}} = \frac{T_c + T_s}{f_c'^{1/4}} = \frac{A_b f_s}{f_c'^{1/4}} = \tag{4}$$

$$\left[59.8 l_d (c_{min} + 0.5 d_b) + 2350 A_b\right]\left(0.1\frac{c_{max}}{c_{min}} + 0.9\right)$$

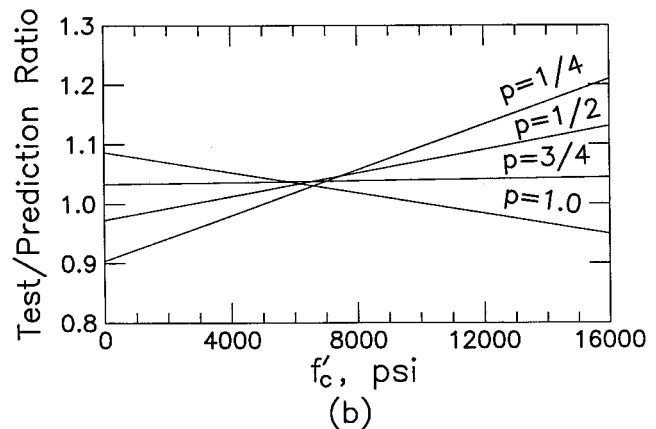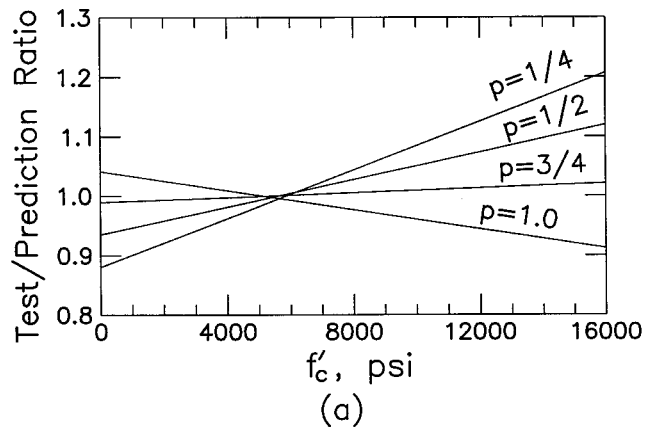$$+ \left(31.14 t_r t_d \frac{NA_{tr}}{n} + 3.99\right) f_c'^{1/2}$$

Fig. 6—Best-fit lines for test-prediction ratios corresponding to powers of f'_c (p = 1/4, 1/2, 3/4, and 1.0), versus compressive strength f'_c: (a) initial comparison; and (b) independent comparison for specimens tested by Kadoriku (1994) (1 psi = 6.89 kPa).

A comparison of the test and predicted strengths for the beams in the database in which the bars are confined by transverse reinforcement is presented in Table A.8 of Appendix A* and Fig. 7. The mean is 1.00, and the COV is 0.115. (By way of comparison, Darwin et al. [1996b] obtained values of 1.01 and 0.125.)

Dropping the intercept 3.99 in Eq. (4), substituting l_d/s for N, where s = stirrup or tie spacing, and solving for development/splice length l_d in terms of A_b and d_b, respectively, gives

$$l_d = \frac{A_b\left[\dfrac{f_s}{f_c'^{1/4}} - 2350\left(0.1\dfrac{c_{max}}{c_{min}} + 0.9\right)\right]}{59.8\left[(c_{min} + 0.5 d_b)\left(0.1\dfrac{c_{max}}{c_{min}} + 0.9\right) + 0.52\dfrac{t_r t_d A_{tr}}{sn}f_c'^{1/2}\right]} \tag{5}$$

$$\frac{l_d}{d_b} = \frac{\dfrac{f_s}{f_c'^{1/4}} - 2350\left(0.1\dfrac{c_{max}}{c_{min}} + 0.9\right)}{76.1\left(\dfrac{c + K_{tr}}{d_b}\right)} \tag{6}$$
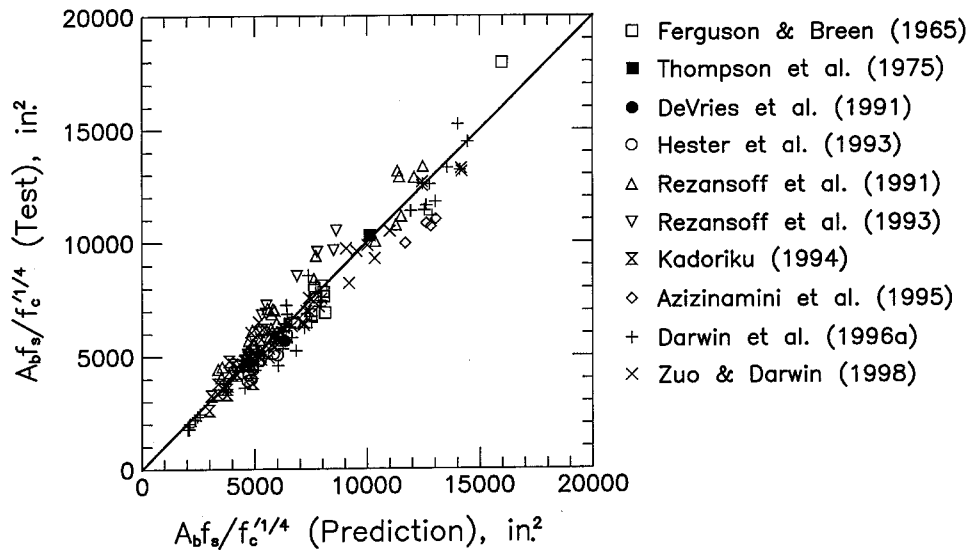
Fig. 7—Experimental bond force $T_b = A_b f_s$ *normalized with respect to* $f_c'^{1/4}$ *versus predicted bond strength, based on Eq. (4) (1 in. = 25 mm).*

in which $K_{tr} = (0.52 t_r t_d A_{tr}/sn) f_c'^{1/2}$, $t_r = 9.6 R_r + 0.28$, $t_d = 0.78 d_b + 0.22$, $l_d/d_b \geq 16$, $c = (c_{min} + 0.5 d_b)(0.1\, c_{max}/c_{min} + 0.9)$ and $(c + K_{tr})/d_b \leq 4.0$. c_{max} and c_{min} are defined following Eq. (1). For conventional bars, the average value of R_r is 0.0727 (Darwin et al. 1996a, 1996b), which allows K_{tr} to be expressed in a somewhat simpler and slightly conservative form as $K_{tr} = (0.5 t_d A_{tr}/sn) f_c'^{1/2}$. The limits on l_d/d_b and $(c + K_{tr})/d_b$ insure that a splitting failure, rather than a pullout failure, will govern bond strength (Darwin et al. 1996b; and Zuo and Darwin 1998).

The final step required to convert Eq. (6) to a design expression involves the application of a strength reduction ϕ factor. Using the LRFD approach described by Darwin et al. (1998), a value of $\phi = 0.90$ is obtained (Zuo and Darwin 1998), matching the value calculated by Darwin et al. (1998) using a smaller database.

Multiplying the right side of Eq. (4) by 0.9, setting $f_s = f_y$, and solving for l_d/d_b gives

$$\frac{l_d}{d_b} = \frac{\dfrac{f_y}{f_c'^{1/4}} - 2100\left(0.1\dfrac{c_{max}}{c_{min}} + 0.9\right)}{68\left(\dfrac{c + K_{tr}}{d_b}\right)} \qquad (7)$$

For design purposes, Eq. (7) can be conservatively simplified by setting $c_{max}/c_{min} = 1.0$ and dropping the 0.25 term in the definition of the effective value of c_{si} (refer to Eq. (1)), which gives

$$\frac{l_d}{d_b} = \frac{\dfrac{f_y}{f_c'^{1/4}} - 2100}{68\left(\dfrac{c + K_{tr}}{d_b}\right)} \qquad (8)$$

Equations (7) and (8) may be applied for bottom-cast developed and spliced bars in normalweight concrete (Darwin et al. 1996b, 1998; and Zuo and Darwin 1998). Because the database used to develop the expressions consists of 90% splice specimens and 10% development length specimens, the 1.3 factor for Class B splices used in ACI 318-99 is not needed. The two equations are similar to the equations developed by Darwin et al. (1996b); the expressions differ in the values of the constants in the numerator and denominator (2100 versus 1900 and 68 versus 72, respectively) and the definition of K_{tr} (Darwin et al. [1996b] used $K_{tr} = 35.5 t_r t_d A_{tr}/sn$). In the earlier work, the 1/4 power of f_c' was used to characterize the effect of concrete strength on T_s, based on a database that included only a small number of specimens cast with high-strength concrete. Because the 1/4 power of f_c' is the same as used to normalize T_c, the earlier K_{tr} term is a function only of bar size, relative rib area, and confining transverse reinforcement. The two values of K_{tr} are equal for $f_c' = 4660$ psi (32 MPa).
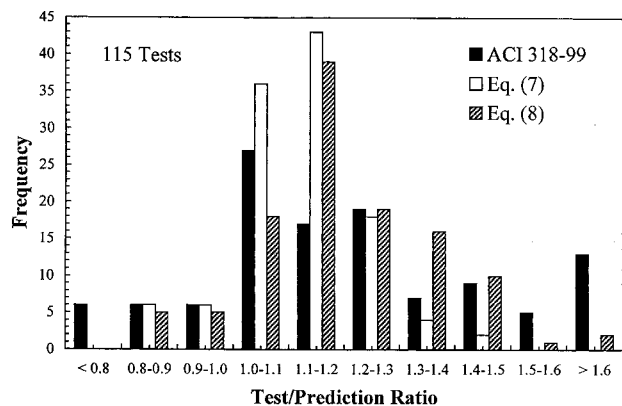
COMPARISON WITH ACI 318-99

Equations (7) and (8) are generally similar in format to Eq. (12-1) in ACI 318-99, which for bottom-cast, uncoated bars in normalweight concrete is

$$\frac{l_d}{d_b} = \frac{3}{40} \frac{f_y}{\sqrt{f_c'}} \frac{\gamma}{\left(\dfrac{c + K_{tr}}{d_b}\right)} \qquad (9)$$

in which $\gamma = 0.8$ for No. 6 (No. 19) and smaller bars and = 1.0 for No. 7 (No. 22) and larger bars, $K_{tr} = A_{tr} f_{yt}/(1500 sn)$, f_{yt} = yield strength of transverse reinforcement, c is as defined for Eq. (8), and $(c + K_{tr})/d_b \leq 2.5$.

The application of Eq. (9) differs from the application of Eq. (7) and (8) in three ways: 1) Eq. (9) distinguishes No. 6 (No. 19) and smaller bars from larger bars using the γ term, leading to a 20% drop in development/splice length for the smaller bars; 2) the K_{tr} term in Eq. (9) includes the yield strength of the transverse reinforcement f_{yt}, even though test results show that f_{yt} has no effect on bond strength; and 3) the development length l_d calculated using Eq. (9) must be increased by 30% for Class B splices (splices in which the area of steel provided is less than two times the area of steel required or where more than 50% of the steel is spliced). l_d in Eq. (9) is used without modification for developed bars and Class A splices (splices for which the area of reinforcement provided is at least twice that required by analysis and 1/2 or less of the total reinforcement is spliced).
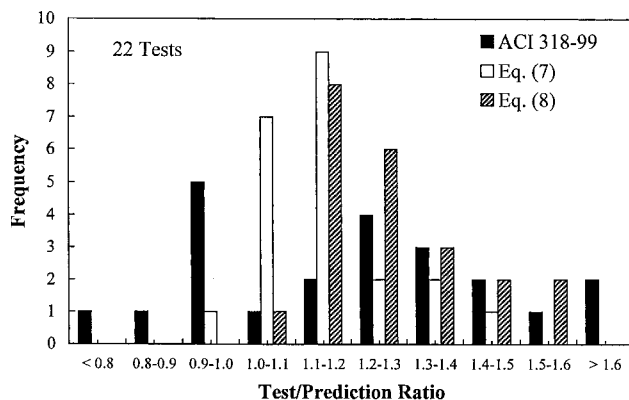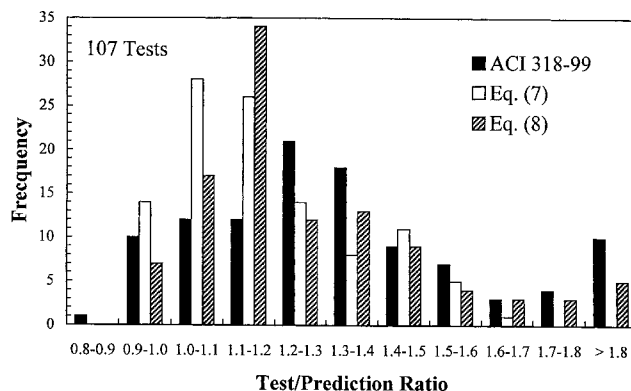
Fig. 8—Comparisons of test-prediction ratio distributions using ACI 318-99, Eq. (7) and Eq. (8) for specimens containing: (a) No. 7 (No. 22) and larger bars; and (b) No. 6 (No. 19) and smaller bars without confining transverse reinforcement.
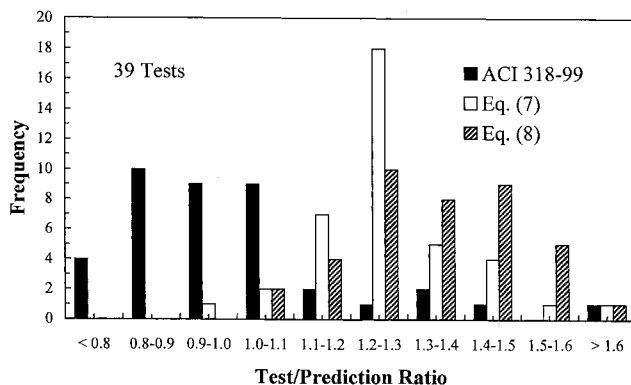
Fig. 9—Comparisons of test-prediction ratio distributions using ACI 318-99, Eq. (7) and Eq. (8) for specimens containing: (a) No. 7 (No. 22) and larger bars; and (b) No. 6 (No. 19) and smaller bars with confining transverse reinforcement.

The relative economy and safety of the ACI criteria and those represented by Eq. (7) and (8) can be obtained by comparing the strengths predicted by the equations with test results in the database maintained by ACI Committee 408. Because of the effect of R_r on K_{tr} (Eq. (7) and (8)), only tests of conventional reinforcement are used for bars confined by transverse reinforcement. The comparisons are presented in Tables A.9 and A.10 of Appendix A[*] and summarized in Table 6 and Fig. 8 and 9. The predicted strengths do not include the 1.3 Class B splice length factor required by ACI 318-99, and the comparisons for Eq. (7) and (8) are made using $K_{tr} = (0.5t_d A_{tr}/sn) f_c'^{1/2}$. Comparisons are limited to test specimens with development/splice lengths ≥ 12 in. and, for bars confined by transverse reinforcement, $l_d/d_b ≥ 16$. Separate results are presented for No. 7 (No. 22) and larger bars and No. 6 (No. 19) and smaller bars to show the effect of the γ factor. Overall, the comparisons with ACI 318 show greater scatter and a significantly greater number of low test-prediction ratios than those obtained with Eq. (7) or (8), especially for No. 6 (No. 19) and smaller bars.

Bars without transverse reinforcement

For No. 7 (No. 22) and larger bars without confining reinforcement (Fig. 8(a)), the test-prediction ratios range from 0.64 to 2.37 for ACI 318, compared with 0.85 to 1.45

for Eq. (7), and 0.85 to 1.73 for Eq. (8). The average test-prediction ratios are 1.22, 1.12, and 1.20, which translates into slightly longer development and Class A splice lengths for ACI 318 than for Eq. (7) and (8). Because of the 1.3 factor, Class B splice lengths are considerably longer for ACI 318. In terms of safety, not only are the lowest test-prediction ratios much lower for ACI 318, but 16% of the test-prediction ratios are less than 1.0, compared with 10 and 9% for Eq. (7) and (8), respectively.

For No. 6 (No. 19) and smaller bars (Fig. 8(b)), the average test-prediction ratios range from 0.78 to 1.78 (mean = 1.22) for ACI 318, from 0.96 to 1.41 (mean = 1.15) for Eq. (7), and from 1.08 to 1.55 (mean = 1.27) for Eq. (8), indicating that, on average, ACI 318 development lengths are between the values for Eq. (7) and (8). In terms of safety, 32% of the test specimens have test-prediction ratios less than 1.0 when evaluated based on ACI 318, compared with 5 and 0% for Eq. (7) and (8), respectively.

Bars with transverse reinforcement

For bars confined by transverse reinforcement, the test-prediction ratios for No. 7 (No. 22) and larger bars (Fig. 9(a)) range from 0.85 to 2.19 (mean = 1.34) for ACI 318, from 0.91 to 1.60 (mean = 1.18) for Eq. (7), and from 0.94 to 1.94 (mean = 1.26) for Eq. (8). In this case, ACI 318 requires greater average development lengths than Eq. (7) or (8). In terms of safety, 10% of the comparisons with ACI 318 have test-prediction ratios below 1.0, versus 13 and 7% for Eq. (7) and (8), respectively.

---

[*]The Appendix is available in xerographic or similar form from ACI headquarters, where it will be kept permanantly on file, at a charge equal to the cost of reproduction plus handling at the time of request.

Table 6—Test-prediction ratios obtained with ACI 318-99 (Eq. (9)) and proposed expressions (Eq. (7) and (8))[*]

		Beams without transverse reinforcement			Beams with transverse reinforcement		
		Test-prediction ratio			Test-prediction ratio		
		$\dfrac{\text{Test}}{\text{ACI 318}}$	$\dfrac{\text{Test}}{\text{Eq. (7)}}$	$\dfrac{\text{Test}}{\text{Eq. (8)}}$	$\dfrac{\text{Test}}{\text{ACI 318}}$	$\dfrac{\text{Test}}{\text{Eq. (7)}}$	$\dfrac{\text{Test}}{\text{Eq. (8)}}$
No. 7 (No. 22) and larger bars	Maximum	2.37	1.45	1.73	2.19	1.60	1.94
	Minimum	0.64	0.85	0.85	0.85	0.91	0.94
	Average	1.22	1.12	1.20	1.34	1.18	1.26
	COV	0.24	0.10	0.14	0.23	0.14	0.18
	Beams with test-pred. < 1.0	16%	10%	9%	10%	13%	7%
No. 6 (No. 19) and smaller bars	Maximum	1.78	1.41	1.55	1.81	1.61	1.61
	Minimum	0.78	0.96	1.08	0.70	0.94	1.07
	Average	1.22	1.15	1.27	1.00	1.27	1.35
	COV	0.22	0.10	0.11	0.21	0.10	0.11
	Beams with test-pred. < 1.0	32%	5%	0%	59%	3%	0%

[*]For specimens with conventional reinforcement in ACI Committee 408 database.

Finally, for No. 6 (No. 19) and smaller bars with confining transverse reinforcement (Fig. 9(b)), the test-prediction ratios range from 0.70 to 1.81 (mean = 1.00) for ACI 318, from 0.94 to 1.61 (mean = 1.27) for Eq. (7), and from 1.07 to 1.61 (mean = 1.35) for Eq. (8). The low average test-prediction ratio for ACI 318 is not a sign of economy, but results from the fact that 59% of the test-prediction ratios are less than 1.0. This compares with 3 and 0% for Eq. (7) and (8), respectively.

Safety and economy

The high percentage of test-prediction ratios less than 1.0 obtained with ACI 318-99 for No. 6 bars and smaller raises significant concerns for the level of safety provided by current design criteria for development/splice length, and demonstrates a lack of justification for using $\gamma = 0.8$ for smaller bars. The comparisons also illustrate that application of Eq. (7) and (8) not only produce, on average, somewhat shorter development lengths and significantly shorter splice lengths than Eq. (9), but that they provide a safety margin that is superior to that provided by the criteria in ACI 318-99.

But why are there no failures?—The question arises as to why failures have not occurred if the safety margin is as low as indicated in this analysis for No. 6 (No. 19) and smaller bars. There are several reasons. First, ACI 318-99 requires that the development lengths calculated using Eq. (9) be increased by 30% for Class B splices. The extra splice length more than makes up for using $\gamma = 0.8$. Second, for developed bars and Class A splices, structures are designed with load factors and capacity reduction factors for flexure, axial load, and shear that provide protection. Third, structures rarely see the values of live load specified in the statutory building codes. Happily, these factors help cushion the effects of the shorter development lengths for the smaller bars. The overall result is a smaller margin of safety for No. 6 (No. 19) and smaller bars than obtained for No. 7 (No. 22) and larger bars. Considering the large percentage of low test-prediction ratios, it would be wise to use $\gamma = 1.0$ for all bar sizes.

SUMMARY AND CONCLUSIONS

Sixty-four splice specimens are used to investigate the effects of concrete properties on the splice strength of high relative rib area and conventional reinforcing bars. Bar relative rib areas range from 0.069 to 0.141. Concrete mixtures with strengths ranging from 4250 to 15,650 psi (29 to 108 MPa) and quantities of limestone and basalt coarse aggregate ranging from 1586 to 1908 lb/yd^3 (941 to 1132 kg/m^3) are used. Test results from this study are combined with the results of previous studies.

Development/splice design equations are developed for uncoated reinforcing bars based on a database including 196 specimens containing bars confined by transverse reinforcement and 171 specimens containing bars not confined by transverse reinforcement. The design equations account for the effects of member geometry, bar size, relative rib area, confinement provided by transverse reinforcement, and concrete strength. A reliability-based strength reduction ϕ factor is incorporated in the design expressions. The design expressions are then compared with the development criteria in ACI 318-99 using the ACI Committee 408 database.

The following conclusions are based on the test results and analyses presented in this paper:

1. Concrete with stronger coarse aggregate provides higher splice strength under all conditions of confinement;

2. For splices confined by transverse reinforcement, the higher the quantity of coarse aggregate in the concrete, the greater the contribution of transverse reinforcement to splice strength;

3. For splices not confined by transverse reinforcement, $f'_c{}^{1/4}$ best characterizes the effect of concrete strength on splice strength. $f'_c{}^{3/4}$ characterizes the effect of concrete strength on the additional splice strength provided by transverse reinforcement;

4. The splice strength of bars confined by transverse reinforcement increases with an increase in relative rib area and bar diameter;

5. The expressions characterizing the splice strength of reinforcing bars presented in this paper accurately represent the development/splice strength of bottom-cast uncoated bars as a function of member geometry, concrete strength, relative rib area, bar size, and confinement provided by both concrete and transverse reinforcement; and

6. The new design expressions are superior to the design criteria in ACI 318-99 in terms of both safety and economy. The criteria in ACI 318-99 for developed bars and Class A splices are unconservative for No. 6 (No. 19) and smaller bars.

REFERENCES

ACI Committee 318, 1999, "Building Code Requirements for Structural Concrete (ACI 318-99) and Commentary (318R-99)," American Concrete Institute, Farmington Hills, Mich., 391 pp.

ASTM A 615/A 615M-95b, 1996, "Standard Specification for Deformed and Plain Billet-Steel Bars for Concrete Reinforcement," *1996 Annual Book of ASTM Standards,* V. 1.04, ASTM, West Conshohocken, Pa., pp. 302-307.

Azizinamini, A.; Stark, M.; Roller, J. H.; and Ghosh, S. K., 1993, "Bond Performance of Reinforcing Bars Embedded in High-Strength Concrete," *ACI Structural Journal,* V. 90, No. 5, Sept.-Oct., pp. 554-561.

Azizinamini, A.; Chisala, M.; Roller, J. H.; and Ghosh, S. K., 1995, "Tension Development Length of Reinforcing Bars Embedded in High-Strength Concrete," *Engineering Structures*, V. 17, No. 7, pp. 512-522.

Barham, S., and Darwin, D., 1999, "Effects of Aggregate Type, Water-to-Cementitious Material Ratio, and Age on Mechanical and Fracture Properties of Concrete," *SM Report* No. 56, University of Kansas Center for Research, Lawrence, Kans., Aug., 95 pp.

Chamberlin, S. J., 1956, "Spacing of Reinforcement in Beams," ACI JOURNAL, *Proceedings* V. 53, No. 1, July, pp. 113-134.

Chamberlin, S. J., 1958, "Spacing of Spliced Bars in Beams," ACI JOURNAL, *Proceedings* V. 54, No. 8, Feb., pp. 689-698.

Chinn, J.; Ferguson, P. M.; and Thompson, J. N., 1955, "Lapped Splices in Reinforced Concrete Beams," ACI JOURNAL, *Proceedings* V. 52, No. 2, Oct., pp. 201-214.

Choi, O. C.; Hadje-Ghaffari, H.; Darwin, D.; and McCabe, S. L., 1991, "Bond of Epoxy-Coated Reinforcement: Bar Parameters," *ACI Materials Journal*, V. 88, No. 2, Mar.-Apr., pp. 207-217.

Darwin, D., and Graham, E. K., 1993, "Effect of Deformation Height and Spacing on Bond Strength of Reinforcing Bars,"*ACI Structural Journal*, V. 90, No. 6, Nov.-Dec., pp. 646-657.

Darwin, D.; Tholen, M. L.; Idun, E. K.; and Zuo, J., 1996a, "Splice Strength of High Relative Rib Area Reinforcing Bars,"*ACI Structural Journal*, V. 93, No. 1, Jan.-Feb., pp. 95-107.

Darwin, D.; Zuo, J.; Tholen, M. L.; and Idun, E. K., 1996b, "Development Length Criteria for Conventional and High Relative Rib Area Reinforcing Bars, " *ACI Structural Journal*, V. 93, No. 3, May-June, pp. 347-359.

Darwin, D.; Idun, E. K.; Zuo, J.; and Tholen, M. L., 1998, "Reliabil-ity-Based Strength Reduction Factor for Bond," *ACI Structural Journal*, V. 95, No. 4, July-Aug., pp. 434-443.

DeVries, R. A.; Moehle, J. P.; and Hester, W., 1991, "Lap Splice Strength of Plain and Epoxy-Coated Reinforcement," *Report* No. UCB/SEMM-91/02, University of California, Berkeley, Calif., Jan., 86 pp.

Esfahani, M. R., and Rangan, B. V., 1996, "Studies on Bond between Concrete and Reinforcing Bars," School of Civil Engineering, Curtin University of Technology, Perth, Western Australia, 315 pp.

Ferguson, P. M., and Breen, J. E., 1965, "Lapped Splices for High-Strength Reinforcing Bars," ACI JOURNAL, *Proceedings* V. 62, No. 9, Sept., pp. 1063-1078.

Hatfield, E.; Azizinamini, A.; and Pavel, R., 1996, "Minimum Stirrup Requirements for Tension Splices in High-Strength Concrete," *Abstract* No. 130, 4th International Symposium on Utilization of High-Strength/High-Performance Concrete, Paris, 10 pp.

Hester, C. J.; Salamizavaregh, S.; Darwin, D.; and McCabe, S. L., 1993, "Bond of Epoxy-Coated Reinforcement: Splices," *ACI Structural Journal*, V. 90, No. 1, Jan.-Feb., pp. 89-102.

Kadoriku, J., 1994, "Study on Behavior of Lap Splices in High-Strength Reinforced Concrete Members," PhD thesis, Kobe University, Mar., Japan, 201 pp.

Kozul, R., and Darwin, D., 1997, "Effects of Aggregate Type, Size, and Content on Concrete Strength and Fracture Energy," *SM Report* No. 43, University of Kansas Center for Research, Lawrence, Kans., June, 83 pp.

Maeda, M.; Otani, S.; and Aoyama, H., 1991, "Bond Splitting Strength in Reinforced Concrete Members," *Transactions of the Japan Concrete Institute*, V. 13, pp. 581-588.

Mathey, R. G., and Watstein, D., 1961. "Investigation of Bond in Beam and Pullout Specimens with High-Yield-Strength Deformed Bars," ACI JOURNAL, *Proceedings* V. 57, No. 9, Mar., pp. 1071-1090

Rezansoff, T.; Konkankar, U. S.; and Fu, Y. C., 1991, "Confinement Limits for Tension Lap Splices under Static Loading," *Report*, University of Saskatchewan, Saskatoon, Sask., Aug., 24 pp.

Rezansoff, T.; Akanni, A.; and Sparling, B., 1993, "Tensile Lap Splices under Static Loading: A Review of the Proposed ACI 318 Code Provisions," *ACI Structural Journal*, V. 90, No. 4, July-Aug. pp. 374-384.

Sakurada, T.; Morohashi, N.; and Tanaka, R., 1993, "Effect of Transverse Reinforcement on Bond Splitting Strength of Lap Splices," *Transactions of the Japan Concrete Institute*., V. 15, pp. 573-580.

Thompson, M.A.; Jirsa, J. O.; Breen, J. E.; and Meinheit, D. F., 1975, "The Behavior of Multiple Lap Splices in Wide Sections," *Research Report* No. 154-1, Center for Highway Research, The University of Texas at Austin, Feb., 75 pp.

Zekany, A. J.; Neumann, S.; and Jirsa, J. O., 1981, "The Influence of Shear on Lapped Splices in Reinforced Concrete," *Research Report* No. 242-2, Center for Highway Research, The University of Texas at Austin, July, 88 pp.

Zuo, J., and Darwin, D., 1998, "Bond Strength of High Relative Rib Area Reinforcing Bars," *SM Report* No. 46, University of Kansas Center for Research, Lawrence, Kans., Jan., 350 pp.